Abstract

Multiple sclerosis (MS) is characterized by lesions in the central nervous system (CNS) consisting of dying mature oligodendrocytes, inflammatory response by immune cells, and subsequent demyelination of axons. Macrophages and other glial cells are essential in response to demyelination, but their role in the remyelination process is only partly known. Previous literature suggests a correlation between CNS remyelination and macrophage appearance at the site of damage. Here, the function of Proline-rich tyrosine kinase 2 (Pyk2), a risk factor tied to neurological diseases including Alzheimer's and Parkinson's, is explored in macrophages and oligodendrocyte precursor cells in terms of MS. Our LFB-PAS histological stainings showed that the initial level of remyelination in *pyk2*$^{-/-}$ mice was significantly higher than that in wild-type mice under cuprizone administration, suggesting Pyk2 has an inhibitory effect on remyelination. In addition, we demonstrated Pyk2 as an important mediator for phagocytosis and signal transduction pathway in macrophage activation. Finally, secretome analysis identified neutrophilic granule protein (Ngp) being suppressed by Pyk2 in post-phagocytosis macrophages, which was further confirmed by Western blots and immunostaining results. Previous report suggests Ngp may subsequently inhibit Cathepsin B (Ctsb), which is thought to be elevated in various types of neurological diseases. By understanding the cellular function of Pyk2 and downstream expression of Ngp and its regulatory pathways, we may explore potential therapeutic candidates curing MS.

Introduction

The majority of cells that make up the central nervous system (CNS) are neuroglial cells, which assist neurons to function properly. Among glial cells, oligodendrocytes are responsible for myelination which insulates the neuronal axons and enhances their action potential transduction efficiency. Myelination starts postnatally and continues into adulthood in both mice and human (Snaidero & Simons, 2014). At times, myelination can be impaired due to external insults and inflammation. In response to demyelination, the CNS activates an endogenous repair process including neuroinflammation, remyelination, and neuroprotection (Karamita et al., 2017). Oligodendrocyte precursor cells (OPCs), originated from the subventricular zone, will migrate to damaged sites where they replace dying oligodendrocytes and remyelinate axons (Menn et al., 2006).

In patients with demyelinating diseases such as Multiple sclerosis (MS), it is believed that such a reparative mechanism deteriorates. Chronic demyelination in MS eventually results in inefficient signal transduction along the axons, eliciting symptoms including weakness, paralysis, and dizziness (Ghasemi et al., 2017). The fundamental cause of MS is unclear, but studies have attributed MS pathogenesis to activation and intrusion of immune cells (mainly B and T lymphocytes), death of oligodendrocytes, and axonal interference (Karamita et al., 2017). B cells were considered to produce proinflammatory cytokines and autoantibodies targeting myelin basic protein, while T cells produce cytotoxic mediators and activate microglia and astrocytes (Jones et al., 2017). Current treatments of MS mainly focus on suppressing immune responses, thereby reducing the number of relapses (Gholamzad et al., 2019); however, such therapies have

no effect on the accumulation of loss of function in progressive MS due to failure of adequate OPC recruitment and differentiation (Kotter et al., 2005; Sim et al., 2002).

Macrophages/microglia were previously believed to be a part of the autoimmune attack in MS, but recent evidence established their importance in remyelination. Prior to remyelination, macrophages/microglia are recruited to site of lesion to initiate debris clearance (Matsushima & Morell, 2001). This is an essential step because myelin debris not only inhibits axonal growth but also impairs subsequent OPC differentiation (Dubois-Dalcq et al., 2005; Kotter et al., 2006; Lampron et al., 2015). As proper debris clearance progresses, macrophages/microglia usher incoming OPCs to differentiate, eventually re-ensheathing damaged axons (Mason et al., 2000). More specifically, recent studies have shown that macrophages/microglia promote OPC differentiation via secretion of factors which includes tumor necrosis factor alpha (TNF-α), insulin-like growth factor-1 (IGF-1), and activin-A (Arnett et al., 2001; Hsieh et al., 2004; Kotter et al., 2005; Miron et al., 2013). In parallel, our previous unpublished data corroborated that OPC differentiation is directly mediated by factors secreted by macrophages that have engulfed apoptotic cells. Given their role in OPC differentiation, macrophages/microglia therefore provide us a plausible approach to enhance remyelination through targeted therapeutic intervention of their secreted factors.

The focus of this study is to explore how proline-rich tyrosine kinase 2 (Pyk2) regulate activities of macrophages/microglia and OPCs in the context of MS. Pyk2, a non-receptor cytoplasmic tyrosine kinase, is known to regulate macrophage processes including motility, differentiation, and bacterial phagocytosis (Paone et al., 2016; UniProt Consortium, 2019). Studies have reported Pyk2 as a risk factor of Alzheimer's disease

and have linked Pyk2 neuropathologically to Parkinson's disease (Lambert et al., 2013; Takahashi et al., 2003). However, Pyk2's role in MS pathogenesis has not been previously reported. An RNA-Seq study on resting state murine CNS mapped Pyk2's expression predominantly in microglia and to a lesser extend in oligodendrocytes and OPCs (Zhang et al., 2014), which led us to speculate Pyk2 may play an important role in macrophages/microglia regulating debris clearance and downstream secretion of factors. To simulate debris clearance process, apoptotic cells (ACs) were used as stimulation for macrophages in this study. Cellular responses caused by ACs are underexplored compared to those of myelin debris, and we believe clearance of ACs is just as critical as myelin clearance prior to remyelination.

Cuprizone model was used in this study. A neurotoxicant, cuprizone mimics the demyelination and remyelination pattern without activating B or T cells, thereby allowing us to study solely the interactions among macrophage/microglia and glial cells (Matsushima & Morell, 2001). During the study, we observed an accelerated remyelination in *pyk2*$^{-/-}$ mice compared to wild-type through LFB/PAS histology. Next, we noticed that deficiency of Pyk2 dramatically impaired phagocytosis of ACs in macrophages. A parallel phosphoproteomics study (data not shown) on macrophages' phagocytosis of ACs revealed phosphorylation of an under-examined site (S747) on Pyk2, and we have generated point-mutated *pyk2* constructs for future testing of this site. To investigate targets in *pyk2*$^{-/-}$ mice that caused accelerated remyelination, we conducted a secretome analysis on post-phagocytosis wild-type and *pyk2*$^{-/-}$ macrophages and identified neutrophilic granule protein (Ngp) as one potential protein normally suppressed by Pyk2. We speculated Ngp is an important mediator of OPC differentiation, and subsequently

corroborated its upregulation in *pyk2*$^{-/-}$ macrophages through immunocytostainings and Western blots. In conclusion, we have not only uncovered a list of secreted factors that potentially contribute to acceleration of remyelination, but also hypothesized a model explaining how macrophages/microglia regulate OPCs and subsequent remyelination through a pathway involving Ngp. Such a model has exciting potentials, as Ngp may prove to be a useful therapeutic target to improve or accelerate remyelination and thereby curing MS.

Materials and Methods

Reagents and Resources	Source	Catalog Number
3% Thioglycollate yeast extract	Matsushima Lab	
Dexamethasone (DEX)	Sigma-Aldrich	D4902
Paraformaldehyde (PFA)	Sigma-Aldrich	P6148
Schiff's fuchsin-sulfite reagent	Sigma-Aldrich	S5133
Hematoxylin Stain Solution, Gill 3	Ricca	3537-32
Solvent blue 38	Sigma-Aldrich	S-3382
Permount Mounting Medium	Thermo Fisher Scientific	SP15-100
CellTracker Green CMFDA Dye	Thermo Fisher Scientific	C2925
CellTracker Orange CMTMR Dye	Thermo Fisher Scientific	C2927
RMPI 1640 Media	Thermo Fisher Scientific	11875-093
RMPI 1640 Media no phenol red	Thermo Fisher Scientific	11835-030
Fetal Bovine Serum (FBS)	Gemini	100-106
VECTASHIELD Hardset Mounting Medium	Vector Lab	H-1500
3xFLAG/Pyk2 Construct	VectorBuilder	
Dimethyl sulfoxide (DMSO)	Sigma-Aldrich	D2650
QIAprep Miniprep kit	Qiagen	27104
QuikChange Mutagenesis kit	Agilent	200515
FuGENE 6	Promega	E269A
VIVASPIN 6 300,000 kDa filters	Sartorius	VS0652
Amicon Ultra 3,000 kDa filters	Millipore	UFC500324

Reagents and Resources	Source	Catalog Number
α-NGP antibody (Rabbit)	Rockland	600-401-GW9S
α-Rabbit IgG Alexa Fluor 488	Invitrogen	A21206
α-Rabbit IgG HRP	Vector Lab	PI-1000
PageRuler Plus Prestained Protein Ladder	Thermo Fisher Scientific	26619
ECL Western Blotting Detection Reagent	Amersham	RPN2232
Protease Inhibitor Cocktail	Sigma-Aldrich	P8340
PhosStop	Roche	4906845001

Mutagenesis Primers

Sequence (5' --> 3')	Identifier	Source
AGCATAGAGTCAGACATCTTTGCGGAGATTCCCGATGAGACC	Y402F	Eurofins Scientific
AATGTGGCCGTCGCCACCTGTAAGAAAGACTGTA	K457A	Eurofins Scientific
CATTGAGGACGAAGACTTTTTCAAAGCCTCTGTGACCCGTC	Y579F/Y580F	Eurofins Scientific
TCTGTGTGCCAGCGCACCTACGCTTA	S747A	Eurofins Scientific

*Underlined indicate targeted amino acids

Mice and cuprizone administration

C57BL/6J (wild-type) mice were purchased from the Jackson Laboratory. *pyk2*$^{-/-}$ mice were a gift from Dr. Michael Schaller (West Virginia University, Morgantown, WV) and were maintained on a C57BL/6J background. All mice were bred and handled under pathogen free conditions by the Matsushima Lab under the protocols approved by the University of North Carolina at Chapel Hill Institutional Animal Care and Use Committee (IACUC).

Cuprizone administration has been previously described (Hiremath et al., 1998). Briefly, 8-10 weeks old mice were fed with a 0.2% w/w cuprizone-containing diet or a control diet for 5 weeks, and subsequently were given control diets ad libitum for a duration ranging from 0 to 3 weeks for remyelination. Mice were perfused with phosphate

buffer containing 4% paraformaldehyde (PFA) and brain samples were harvested and coronally sectioned at 5µm. Both male and female mice were used in the experiments since no obvious difference between sexes under cuprizone administration was previously observed (Taylor et al., 2010).

Luxol fast blue/periodic acid Schiff (LFB-PAS) staining

LFB-PAS stainings were performed as previously described (Arnett et al., 2002). Briefly, 4% PFA-fixed 5µm coronal brain sections on slides were dehydrated, incubated overnight at 60°C in 0.2% Solvent Blue 38 and dipped in 70% ethanol to wash off excessive stainings. Sections were then stained with Periodic acid-Schiff (PAS) and Gill 3 hematoxylin. Slides were then dehydrated and mounted in Permount. LFB-PAS stained slides were then graded in a double-blind fashion, and the level of myelination was rated on a three-point scale, with higher scores representing better myelination.

Preparation of macrophages

Thioglycollate-elicited macrophages were obtained as previously described (Scott et al., 2001). Briefly, 8-12 weeks old mice were intraperitoneally injected with 3 mL of 3% thioglycolate prior to harvest by peritoneal wash in Versene. Peritoneal exudate cells (PECs) were washed 3 times in PBS prior to resuspension in RPMI with 5% FBS. For phagocytosis assays of apoptotic cells (ACs), PECs were plated on Poly-D-Lysine coated coverslips in 24-well plates at a density of 1.5×10^5 cells/well. For lysate and supernatant collection purposes, PECs were plated in 100 mm dishes at a density

of $1x10^7$ cells/dish. PECs were allowed to adhere overnight at 37 ºC 5% CO_2 and were subsequently washed to retained only macrophages.

Inducing apoptotic cells

ACs were harvested as previously described (Seitz et al., 2007). Briefly, thymi from 4-6 weeks old wild-type mice were harvested and tissues were mechanically dissociated using forceps. Cells were then washed and incubated in RPMI 1640 media with 5% FBS containing 2µM dexamethasone (DEX) at a density of 5×10^6 cells/mL in a 37 ºC water bath for 4 hours. During the incubation, a gentle agitation was performed every hour to ensure even distribution of DEX. For imaging phagocytosis, ACs were washed with PBS to remove DEX and were stained with 2µM CellTracker Green after 2.5 hours of incubation prior to resuspension in RPMI 1640 with 5% FBS. For collecting macrophage lysates and supernatants, ACs were washed with PBS to remove DEX after 3.5 hours of incubation prior to resuspension in RPMI 1640 with 5% FBS.

Phagocytosis of apoptotic cells

24-hour post-plating macrophages were stained with CellTracker Orange prior to ACs stimulation at a 10:1 ratio of AC: macrophage. After 30 minutes of macrophage stimulation at 37 ºC, wells were washed repeatedly with PBS until no free-floating ACs were observed. Cells were then fixed with 1% PFA for 15 minutes, and the coverslips were placed onto microscope slides with Vectashield. Immunostainings were viewed with ZEN software on Zeiss LSM 780 confocal microscope to obtain z-stack images.

Macrophages were then counted to determine the percentage of phagocytosis based on whether their fluorescent signals overlap with those of ACs (procedural flowchart in Figure 1).

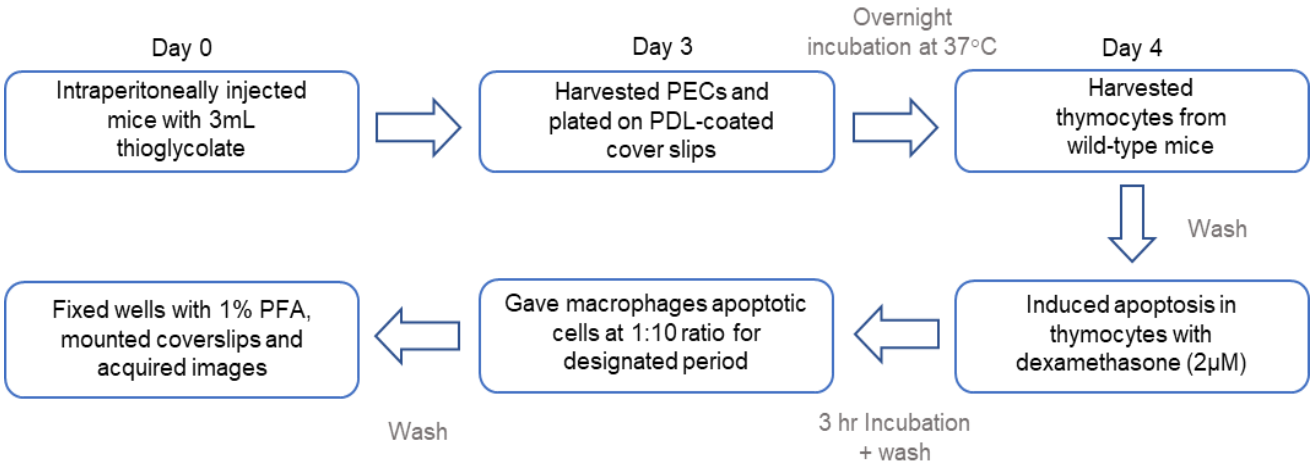

Figure 1. Flowchart of the phagocytosis of apoptotic cells assay procedure.

Cloning and directed mutagenesis

3xFLAG/murine Pyk2 construct was purchased from VectorBuilder. Constructs encoding various point mutations on *pyk2* were generated by QuikChange site-directed mutagenesis kit. Briefly, 3xFLAG/Pyk2 wild-type plasmids were extracted using Maxiprep kit and were amplified in PCR according to manufacturer's protocol. Samples were then sequenced (Eton Bioscience) to ensure successful mutagenesis prior to amplification in bacteria. Constructs containing mutated Pyk2 were collected using miniprep and stored at -20 ºC for future use.

Supernatant collection of activated macrophages

24-hour post-plating macrophages were stimulated by ACs at a 10:1 ratio of AC: macrophage. After 30 minutes of macrophage stimulation at 37 ºC, dishes were washed repeatedly with PBS until no free-floating ACs were observed. Macrophages were incubated in RPMI phenol-free media overnight at 37 ºC prior to supernatant collection, and supernatants were subsequently concentrated using VIVASPIN 6 and Amicon Ultra filters following manufacturers' protocols. Samples were then prepared and analyzed by the UNC Proteomics Core Facility.

Sample preparation for LC-MS/MS analysis

The concentrated supernatants were denatured with 7M urea, reduced with 5mM DTT for 30 minutes at 37°C, then alkylated using 15 mM iodoacetamide for 30 min at room temperature. Each sample was then diluted to 0.5M Urea with 50 mM ammonium bicarbonate and digested with trypsin (1:50) overnight at 37°C. Digestion was quenched by acidifying to pH <2 and desalted using Thermo Pierce C18 spin columns. Peptides were quantified using the Pierce Colorimetric Peptide Quantitation Kit.

LC-MS/MS analysis and data processing

Samples (1 µg) were analyzed by LC-MS/MS using a Thermo Easy nLC 1200 coupled to an Orbitrap QExactive HF mass spectrometer equipped with an EasySpray nano source. Samples were loaded onto an EasySpray C18 column (75 µm ID X 25cm, 2 µm particle size) and eluted over a 90 min method. The gradient for separation consisted 5-40% B at a 250 nl/min flow rate, where mobile phase A [water, 0.1% formic ac-

id] and mobile phase B [80% acetonitrile, 0.1% formic acid]. The QExactive HF was operated in data-dependent mode where the 15 most intense precursors were selected for subsequent fragmentation. Resolution for the precursor scan (m/z 350–1700) was set to 60,000 with a target value of 3×10^6 ions, 100 ms max IT. MS/MS scans resolution was set to 15,000 with a target value of 1×10^5 ions, 60 ms max IT. The normalized collision energy was set to 27% for HCD. Dynamic exclusion was set to 30 s and precursors with unknown charge or a charge state of 1 and ≥ 7 were excluded.

Raw data were processed using the MaxQuant software suite (version 1.6.1.0) for protein identification and label-free quantitation (Cox & Mann, 2008; Cox et al., 2011). Data were searched against a Uniprot mouse database using the integrated Andromeda search engine. A maximum of two missed tryptic cleavages were allowed. The fixed modification specified was carbamidomethylation of cysteine residues and the variable modification specified was oxidation of methionine. Match between runs was enabled. Results were filtered to 1% FDR at the unique peptide level and grouped into proteins within MaxQuant (Cox et al., 2014). Only proteins with >1 unique+razor peptide were used for label-free quantitation. Statistical analyses (ANOVA, Student's t-test) were performed in Perseus software.

Immunocytochemistry

Macrophages on coverslips were fixed with 1% PFA for 15 minutes. After blocking with 5% milk, samples were incubated with α-Ngp antibody (1:200) for 1 hour at room temperature. Proteins were then visualized with α-Rabbit IgG Alexa Fluor 488

(1:1000) and placed onto microscope slides with Vectashield. Immunofluorescence stainings were captured with ZEN software on Zeiss LSM 780 confocal microscope and quantified using ImageJ.

Western blots

Cell lysates were prepared in lysis buffer consist of 0.1% NP-40, 50mM Tris-HCl (pH = 8), 150mM NaCl, 2mM EDTA, 1,10-phenanthroline, and 2x protease inhibitor cocktail (Sigma). 25 ug of lysate samples were separated on 10% SDS-PAGE gel and transferred to nitrocellulose membranes. After blocking with 5% milk, membranes were washed and incubated with α-Ngp antibody (1:1000) overnight at 4°C. Proteins were then detected with α-Rabbit IgG HRP (1:10000) and visualized using ECL kit. Western blot images were subsequently captured with Amersham Imager 600 and quantified using ImageJ.

Statistical analysis

Data are expressed as mean ± SE. Statistical analysis of different groups was performed by Student's test as indicated. $P < 0.05$ was considered significant. All statistical calculations were performed using Graphpad PRISM.

Results

Pyk2-Deficient Mice Demonstrate Accelerated Remyelination

To determine the effect of Pyk2 in cuprizone-induced demyelination of corpus callosum, *pyk2*$^{-/-}$ and wild-type mice were fed 0.2% w/w cuprizone diet for 5 wk, and corpus callosum sections over a time course were collected and stained with LFB/PAS (representative stainings in Figure 2A). Myelination levels were quantified in a double-blind fashion. By 5 wk, sections of both *pyk2*$^{-/-}$ and wild-type mice showed almost full demyelination, as indicated by the scores near zero (Figure 2B). However, myelination levels ensued with the subsequent removal of cuprizone were significantly ($p < 0.05$) greater in the *pyk2*$^{-/-}$ mice (1.57 ± 0.26) compared to wild-type mice (0.74 ± 0.19) treated at 5+1 wk (Figure 2B). The results demonstrate that the deficiency of Pyk2 causes an accelerated remyelination while not affecting demyelination in the corpus callosum.

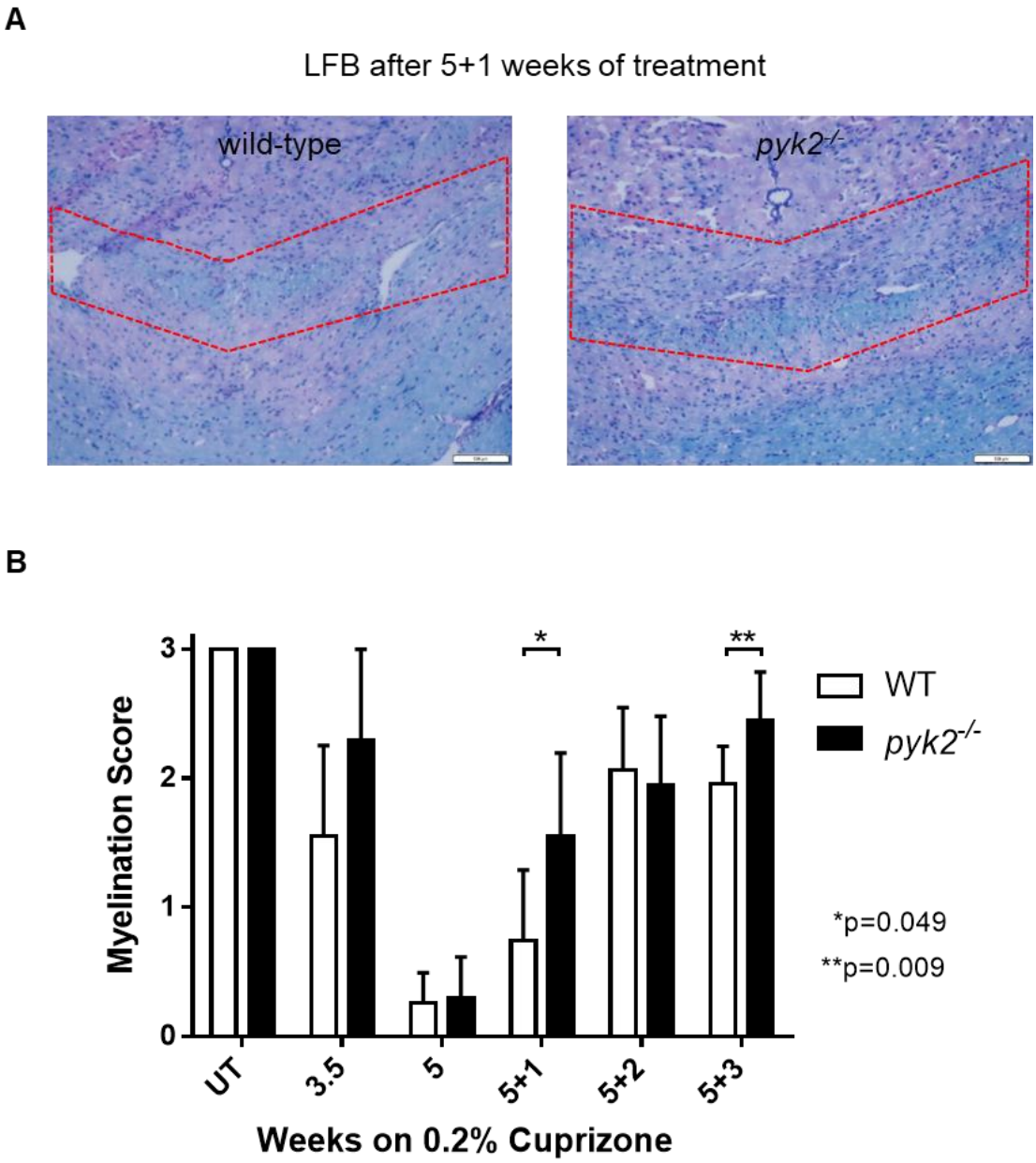

Figure 2. *pyk2*$^{-/-}$ mice show accelerated remyelination compared with wild-type mice in the corpus callosum after cuprizone treatment. A, LFB-PAS stained coronal brain sections of corpus callosum from WT and *pyk2*$^{-/-}$ mice at 5+1 wk. Corpus callosum areas were indicated in red. Scale bar = 100 μm. B, quantification of the myelination levels in corpus callosum. Stained sections were assessed in a double-blind fashion, and the levels of myelination were rated on a three-point scale. Higher scores represent greater levels of myelination. *pyk2*$^{-/-}$ mice show statistically significant increases in remyelination at 5+1 ($p < 0.05$) and 5+3 wk ($p < 0.01$) by Student's t-test. $n \geq 6$ for all treatment groups. UT = untreated.

Pyk2 is Required for Phagocytosis of Apoptotic Cells by Macrophages

To assess Pyk2's role, *pyk2*$^{-/-}$ and wild-type macrophages were stimulated with ACs to trigger phagocytosis. Macrophages and ACs were labeled with different fluorescent tags, and the quantification of the percentages of macrophages (orange) that ingested ACs (green) was based on the overlapping of their respective fluorescent signal (representative images in Figure 3A; schematic drawing in Figure 3B). In absence of Pyk2, a significant impairment ($p < 0.01$) in macrophages' ability to ingest ACs was observed (10.4 ± 0.9%) compared to that in wild-type (26.7 ± 1.5%) (Figure 3C). The results demonstrate that Pyk2 is necessary for proper macrophage phagocytosis of ACs.

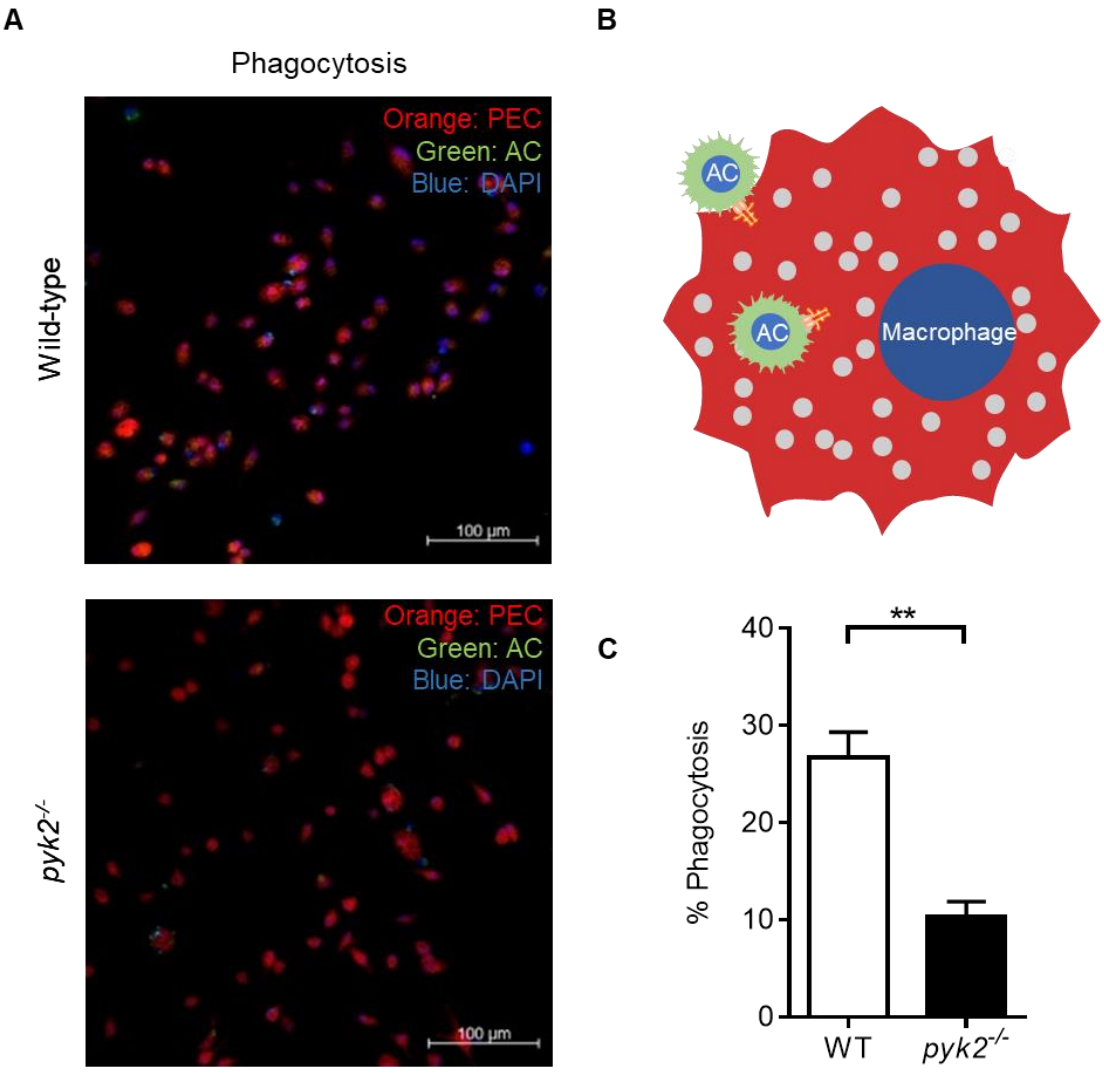

Figure 3. pyk2 is an important mediator of phagocytosis of apoptotic cells by macrophages. A, Confocal images of phagocytosis of ACs (10:1 ACs to macrophages) by wild-type (WT) and *pyk2*$^{-/-}$ macrophages. Macrophages were labeled orange, ACs were labeled green, and cell nuclei were labeled blue with DAPI. Z-stack images were acquired using Zeiss LSM 780 confocal microscope. Scale bar = 100 μm. B, visual representation of overlapping of fluorescent signals during phagocytosis in 3A. Colors correspond to those in 3A. C, quantification of ingestion of ACs by WT and *pyk2*$^{-/-}$ macrophages. At least 250 macrophages of each replicate were counted. n = 4. **p < 0.01, Student's t-test.

Pyk2 Mutant Variant Constructs

S747 on Pyk2, an under-examined phosphorylation site, was phosphorylated in macrophages during phagocytosis of ACs in a parallel phosphoproteomics study (data not shown). Since we proved Pyk2's regulation of macrophage phagocytosis of ACs, we speculated that S747 on Pyk2 is responsible for phagocytosis' downstream signaling events leading to secretion of factors that affect OPC differentiation. To address this question, we have purchased a construct containing *pyk2* gene (Figure 4) and S747A mutagenesis primer to generate S747A *pyk2* construct. In addition, mutagenesis primers targeting sites (Y402F, K457A, and Y579F/Y580F) responsible for Pyk2's kinase activity were purchased to test whether the secretion of differentiation factors is independent of Pyk2's kinase activity. We have generated several mutant variants of *pyk2* so far, including S747A and Y402/Y579F/Y580F. The ongoing next step is to transfect a murine microglial cell line, BV-2. For negative control, lentiviral *pyk2* shRNA clones were obtained from the UNC Lenti-shRNA Core Facility and will be used on BV-2. The resulting stable BV-2 clones with different variants of Pyk2 expressions will allow us to

assess what phosphorylation sites on Pyk2 are responsible for phagocytosis and for secretion of factors post-phagocytosis in a murine cell line.

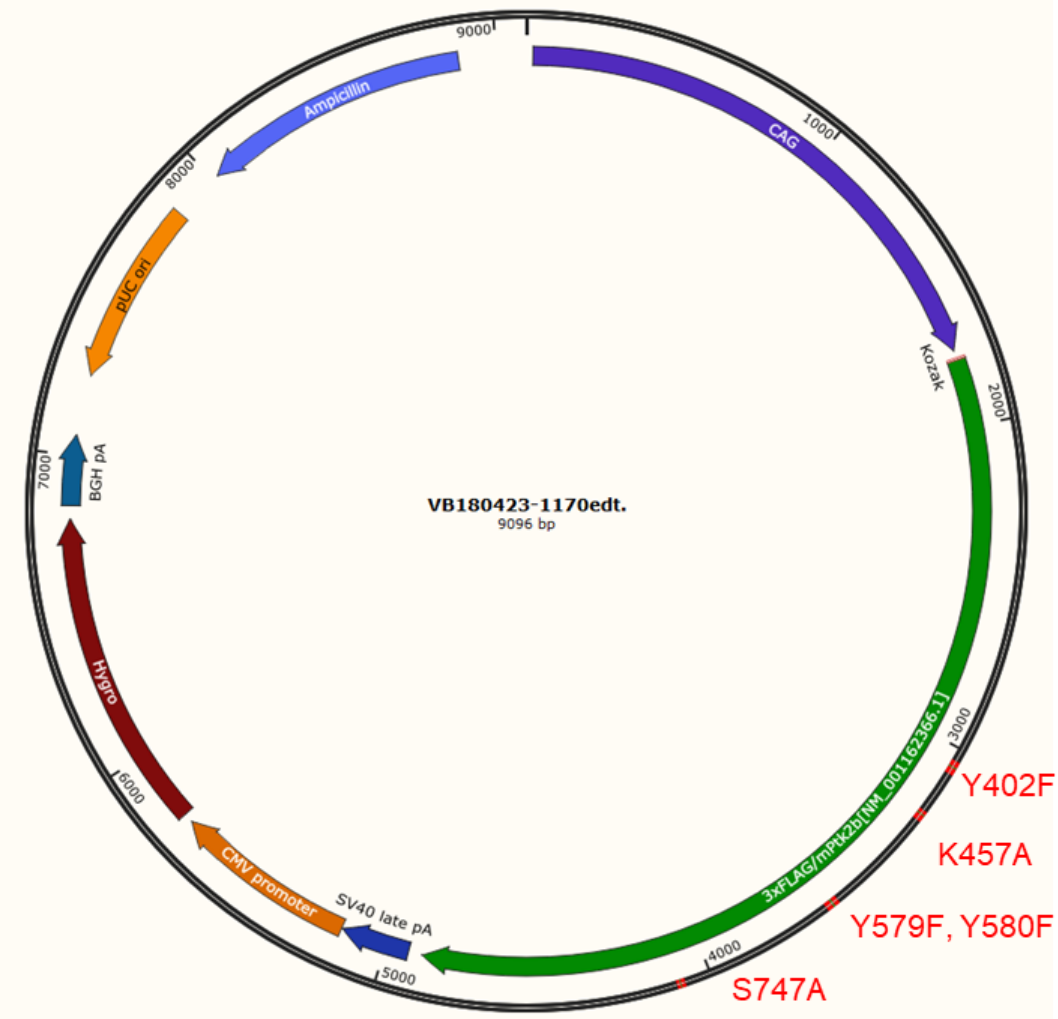

Figure 4. wild-type pyk2 gene construct. A construct containing murine *pyk2* (mPtk2b). *pyk2* fused with 3x*FLAG* gene for visualization and immunoprecipitation purposes. Hygromycin resistance gene was incorporated for antibiotic selection purpose. Targeted phosphorylation sites were labeled on the construct in green, contained in regions of mutagenesis primers in red.

Secretome Analysis of Macrophages Stimulated by Apoptotic Cells

Unpublished data from previous lab members has shown that macrophages provide OPCs with extracellular factors that induce activation, growth, and differentiation. Since *in vivo* LFB-PAS histology has demonstrated that the deficiency of Pyk2 resulted in faster remyelination, factors secreted in *pyk2*$^{-/-}$ macrophages were speculated to stimulate OPC proliferation and differentiation. Here, the secreted factors from post-phagocytosis *pyk2*$^{-/-}$ and wild-type macrophages were identified and analyzed by the UNC Proteomics Core Facility (procedural flowchart shown in Figure 5A). Out of the 1,000 proteins filtered and quantified, Student's t-test ($p < 0.05$) resulted in 37 statistically significant candidates (Figure 5B).

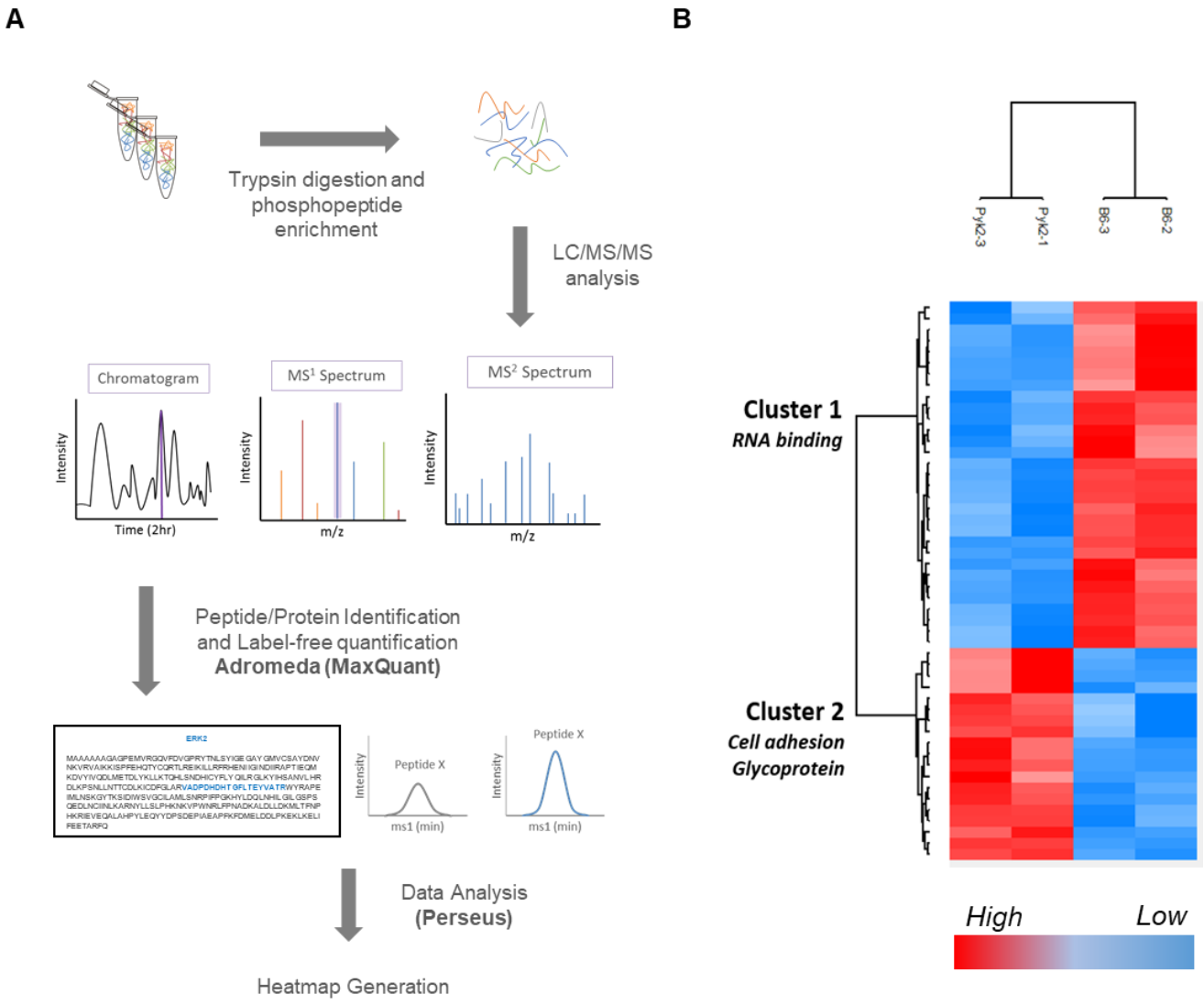

Figure 5. Secretome profile of post-phagocytosis Macrophages reveals potential mediators of phagocytosis. Supernatants of wild-type (WT) and *pyk2*$^{-/-}$ macrophages were collected 24 hr post-phagocytosis of ACs and were analyzed by the UNC Proteomics Core Facility. A, proteomics workflow. Samples were digested and enriched prior to LC/MS/MS analysis. Proteins were then identified and quantified using MaxQuant software. Heatmap was subsequently generated using Perseus. B, heatmap of secreted proteins in WT (B6) and *pyk2*$^{-/-}$ macrophages. Student's t-test revealed 37 proteins that showed significantly different expression levels between WT and *pyk2*$^{-/-}$ secretome profiles (Red = high; Blue = low). Proteins were categorized under two clusters by their generic functions.

Secreted proteins were categorized into two clusters based on their respective expression levels represented by LFQ intensities. Cluster 1 represents secreted proteins upregulated in *pyk2*$^{-/-}$ macrophages responsible mainly for RNA binding, while cluster 2 represents those upregulated in wild-type macrophages responsible for cell adhesion. Among the secreted factors upregulated in *pyk2*$^{-/-}$ macrophages, neutrophilic granule protein (Ngp), a cysteine-type endopeptidase, was identified to be the top candidate, showing a 7.30-fold upregulation compared to its level in wild-type macrophages (Table 1). The significant upregulation of Ngp suggests itself a strong candidate for accelerated remyelination in *pyk2*$^{-/-}$ mice.

	Protein names	Gene names	*pyk2*$^{-/-}$ vs. wild-type, LFQ Ratio
Cluster 2	Neutrophilic granule protein	Ngp	7.30
	Serine hydroxymethyltransferase 1	Shmt1	6.54
	Serpin Family F Member 1	Serpinf1	2.44
	Tartrate-resistant acid phosphatase 5	Acp5	2.14
	Tissue alpha-L-fucosidase	Fuca1	1.98
Cluster 1	Talin-1	Tln1	0.52
	Acyl-CoA thioesterase 2	Acot2	0.48
	GTP-binding nuclear protein Ran	Ran	0.47
	Antileukoproteinase	Slpi	0.41
	Signal recognition particle 9	Srp9	0.20

Table 1. Top 5 protein candidates upregulated in 24 hr post-phagocytosis wild-type and pyk2$^{-/-}$ macrophages. Refer to Figure 5. Label-free quantification (LFQ) intensity of proteins were obtained using MaxQuant, and the LFQ ratios of proteins in wild-type and *pyk2*$^{-/-}$ macrophages were subsequently calculated. Top 5 most upregulated proteins in *pyk2*$^{-/-}$ (Cluster 2) and wild-type macrophages (Cluster 1) were listed here.

Pyk2 Regulates Ngp Expression in Macrophages

To investigate further, a time course study of Ngp expression in *pyk2*$^{-/-}$ and wild-type macrophages was performed to corroborate the secretome findings and to determine the time point where Ngp is upregulated in absence of Pyk2. Macrophages 6 and 18 hr after ACs stimulation were assessed by immunocytochemistry and Western blot.

For immunostaining, macrophages were fixed with 1% PFA and immunostained for Ngp (Green) prior to image capture. Levels of Ngp expression present in wild-type and *pyk2*$^{-/-}$ macrophages post-phagocytosis were subsequently quantified by integrated density. A decrease of Ngp level in wild-type and an increase of Ngp level in absence of Pyk2 were observed compared to their respective controls in 18 hr post-phagocytosis macrophages (Figure 6A, B). No visual difference was observed in 6 hr post-phagocytosis macrophages (Figure not shown). We speculate the resemblance of Ngp level at 6 hr was due to insufficient time of Ngp transcription and translation.

For Western blot, macrophage lysates were harvested and ran on a 10% SDS-PAGE gel. Ngp levels of all samples were subsequently detected and normalized to their respective β-actin levels prior to normalization to the Ngp level of WT control. By 18 hr post-phagocytosis, intracellular level of Ngp was suppressed in wild-type macrophages to half-fold but elevated in *pyk2*$^{-/-}$ macrophages to 2-fold (Figure 6C, D). In conclusion, immunostaining and Western blot results demonstrated the elevation of Ngp production in *pyk2*$^{-/-}$ macrophages compared to wild-type macrophages, validating the secretome findings of the same elevation of Ngp secretion pattern.

A

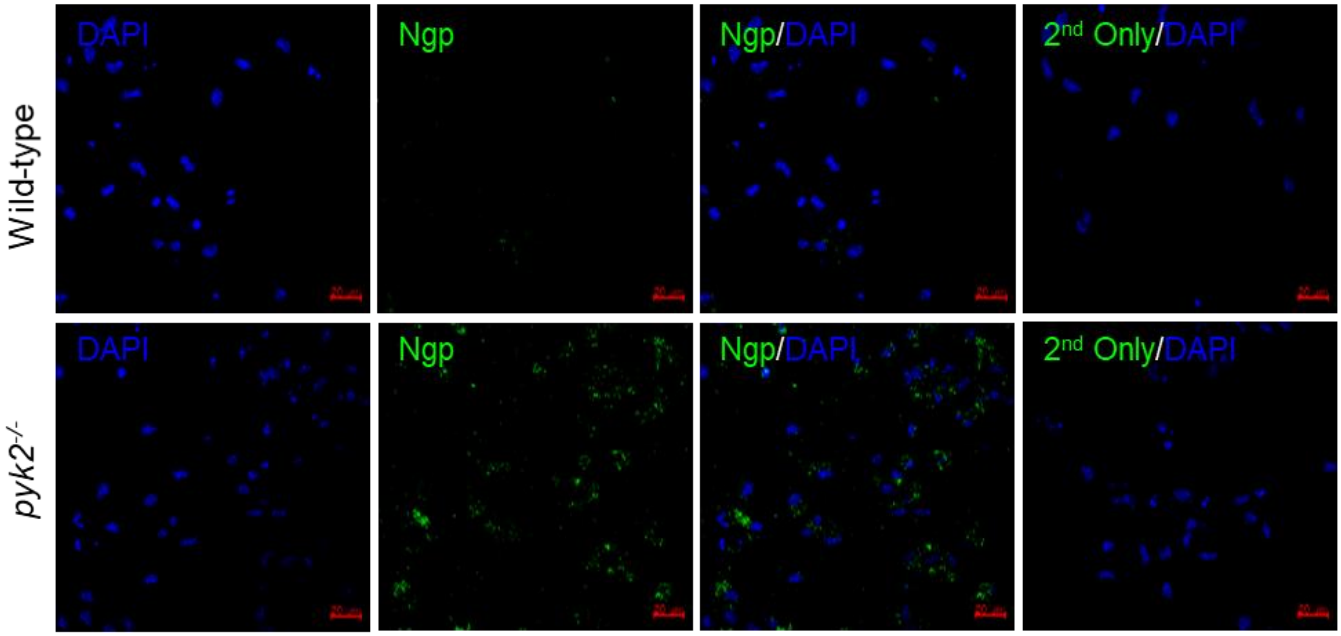
DAPI
Ngp
Ngp/DAPI
2nd Only/DAPI
Wild-type
DAPI
Ngp
Ngp/DAPI
2nd Only/DAPI
pyk2-/-

B

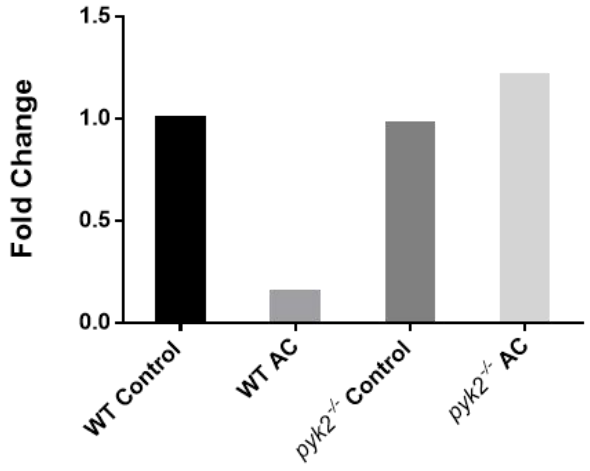
Fold Change
1.5
1.0
0.5
0.0
WT Control
WT AC
pyk2-/- Control
pyk2-/- AC

C

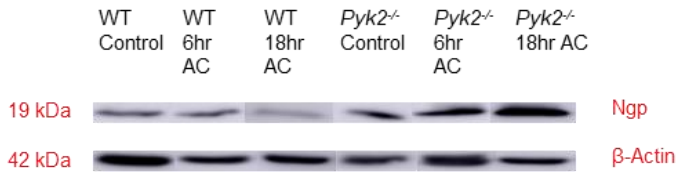
WT Control
WT 6hr AC
WT 18hr AC
Pyk2-/- Control
Pyk2-/- 6hr AC
Pyk2-/- 18hr AC
19 kDa
Ngp
42 kDa
β-Actin

D

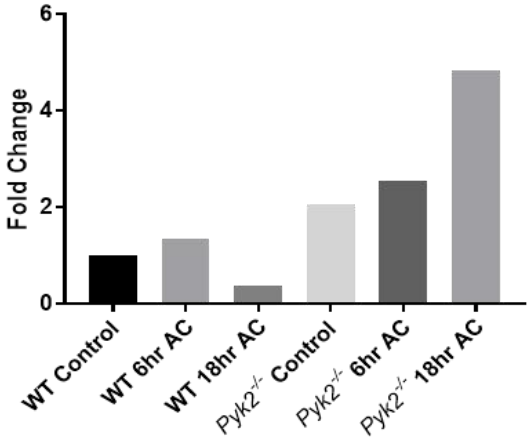
Fold Change
6
4
2
0
WT Control
WT 6hr AC
WT 18hr AC
Pyk2-/- Control
Pyk2-/- 6hr AC
Pyk2-/- 18hr AC

Figure 6. Pyk2 regulates level of Ngp in post-phagocytotic macrophages. Wild-type (WT) and *pyk2*$^{-/-}$ macrophages were stimulated with ACs prior to experiments. A, immunostaining of Ngp in WT and *pyk2*$^{-/-}$ macrophages 18hr post ACs stimulation. Cells were fixed with 1% PFA for 15 mins prior to staining. Green = Ngp, and blue = DAPI. Scale bar = 20 μm. B, quantification of intracellular Ngp fluorescence. Fluorescence intensities normalized to that of WT control. C, Western blot of Ngp in lysates from WT and *pyk2*$^{-/-}$ macrophages 6 and 18 hr post ACs stimulation. Controls did not receive stimulation and were collected at 6 hr time point. D, quantification of intracellular level of Ngp in lysates. Ngp levels were normalized to β-actin levels, followed by normalization to WT control. A decrease in Ngp level in WT macrophages and an increase in *pyk2*$^{-/-}$ macrophages were observed in both 6B and 6D.

Discussion

We have demonstrated in this study that AC-induced macrophage activation pathway is Pyk2-mediated. This is important in the context of MS, as Pyk2 is now tied to a necessary process during MS pathogenesis, providing us a new perspective. On the other hand, the complete depletion of Pyk2 leads to accelerated remyelination in the murine CNS, possibly through regulating secretion of Ngp and suppressing other factors detrimental to OPC differentiation.

We suspect that the dual roles of Pyk2 in phagocytosis and secreting of factors are partly due to Pyk2 expression in OPCs, which was not addressed in this study. As stated earlier, an RNA-Seq study showed that Pyk2 is expressed in OPCs in a resting murine brain (Zhang et al., 2014); however, Pyk2's protein expression levels among the glial cells have yet to be established, especially in the context of MS. Our immediate next step is therefore to conduct an immunohistostaining, colocalizing Pyk2 with microglia and OPCs respectively at 5+1 wk of cuprizone in wild-type mice. The result will give us a more direct view of whether Pyk2 has a bigger role in OPCs themselves during MS pathogenesis.

The phosphoproteomics study demonstrated that phosphorylation of S747 on Pyk2 is significantly impeded during phagocytosis when a major phagocytosis receptor is knocked out from macrophages (data not shown). S747 of Pyk2 has been previously implicated as part of the nuclear targeting sequence of Pyk2, which assists in nuclear localization (Faure et al., 2013). We speculate that the internalization of apoptotic cells during phagocytosis inhibits transcription of factors for OPC differentiation that is mediated briefly by Pyk2. Combined with the fact that *pyk2*$^{-/-}$ mice demonstrated accelerated remyelination, a potential key link where Pyk2 may inhibit remyelination lies in its ability to regulate phosphatases and subsequent downstream signal transduction. Thus, the position of Pyk2 in regulating signal transduction and reparative pathways warrants further investigation. We have already generated plasmids with mutant Pyk2 variants, and we will transfect murine microglial BV-2 cells to test whether S747 is responsible for regulating secretion of factors beneficial to OPC differentiation.

After literature searches on factors identified in secretome analysis, we believe Ngp could be a likely therapeutic target for MS. Ngp was reported as a cathepsin B (Ctsb) inhibitor (Boutté et al., 2011), which is a lysosomal cysteine protease necessary in immune response and cell turnover (Mort & Buttle, 1997). Specifically, increased levels of Ctsb activity were observed in brains and peripheral blood macrophages of MS patients (Bever & Garver, 1995; Bever et al., 1994). Furthermore, the literature suggested cysteine proteases could serve as therapeutic targets for neurological diseases including Alzheimer's, multiple sclerosis, and brain traumatic injuries (Haves-Zburof et al., 2011; Hook et al., 2015; Siklos et al., 2015). In addition, Pyk2 deficiency leads to inefficient neutrophil degranulation (Kamen et al., 2011). The findings further validate our

speculation that the absence of Pyk2 would permit Ngp to ameliorate the proteolytic activities in the extracellular environment. To support our point, we will need to quantify the amount of Ngp and Ctsb as well as colocalizing these proteins with microglia during our cuprizone administration time course.

Aside from Ngp, other upregulated protein candidates in *Pyk2*$^{-/-}$ macrophages were also inspected. Shmt1 is a cellular response to leukemia inhibitory factor (LIF), which is an IL-6 cytokine that induces cell differentiation; Serpinf1 induces extensive neuronal differentiation and inhibits endopeptidase activity; and Acp5 inhibits inflammatory response by negatively regulating IL-12 and IL-1β production (Uniprot Consortium, 2019). Thus, these other secreted factors by *pyk2*$^{-/-}$ secretome may augment the reparative process. We observed that even though these proteins have not been upregulated as much as Ngp had, they uniformly exhibit functions including cell differentiation and anti-inflammation; therefore, these proteins are also worth studying in the future.

Taken collectively, we have proposed a model describing interaction between macrophages/microglia and OPCs during remyelination through Pyk2 and Ngp (Figure 7). Upon macrophages binding and phagocytizing apoptotic cells, Pyk2 becomes phosphorylated at S747 and migrates inside the nucleus of activated macrophages. pPyk2 inhibits the transcription of Ngp as well as other potential differentiation factors through an unknown mechanism, indirectly allowing for Ctsb proteolytic activities in area of lesion and delaying remyelination; however, in absence of Pyk2 phosphorylation of S747, phagocytosis proceeds normally in macrophages, but Pyk2 no longer translocate to the nucleus. Transcription of Ngp and differentiation factors are no longer suppressed, and Ngp is secreted to inactivate Ctsb released by own macrophage and other neighbors

while differentiation factors are given to OPC to instruct differentiation. Such a model is still rudimentary and requires extensive testing. As we address questions within the model, an important issue remains unresolved and require further study. For example, what is Pyk2's involvement in phagocytosis of myelin-stimulated macrophages. Lastly, Pyk2 may have dual roles in macrophages where we will need to stimulate macrophages with both ACs and myelin as this condition will more accurately reflect the events during MS pathogenesis.

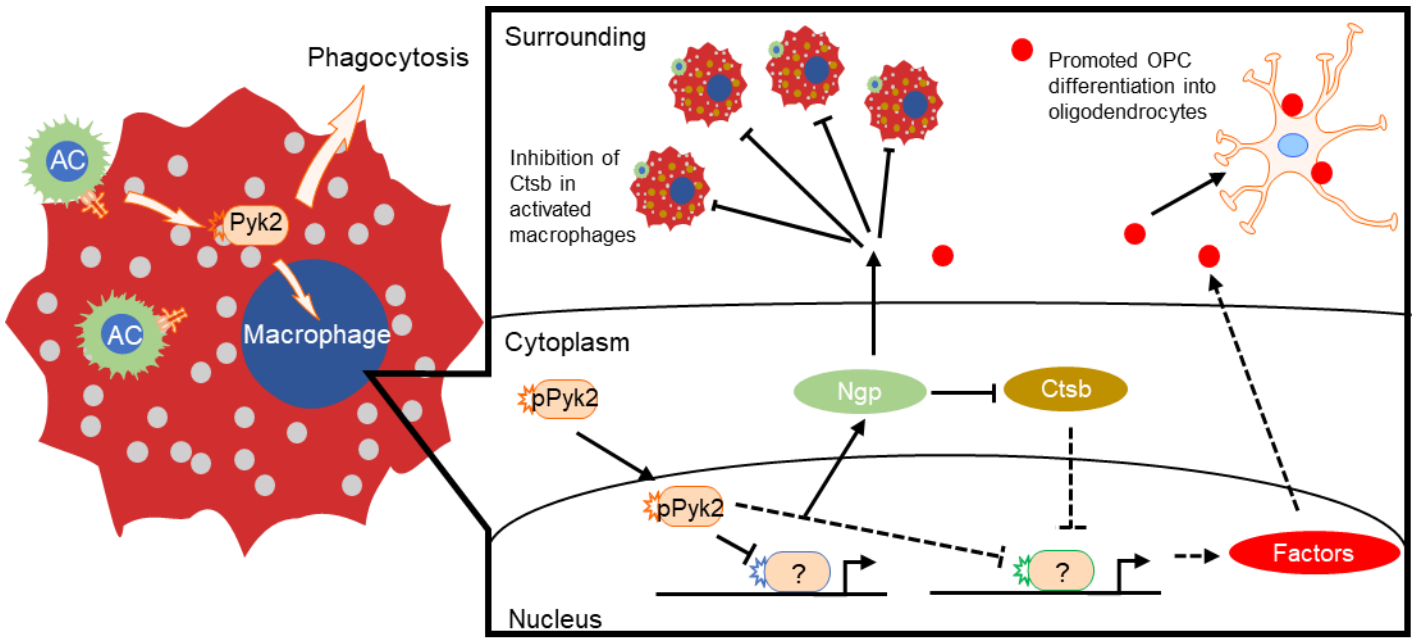

Figure 7. Proposed model of Pyk2-mediated pathway in macrophages.

Acknowledgement

I would like to thank my thesis advisor and principle investigator Dr. Glenn Matsushima for teaching me and guiding me throughout the project, Dr. Laura Herring for processing the proteomics data, Akhil Patel, Dr. Naoki Nakagawa, Dr. Keiko Nakagawa and Dr. Nagu Muthusamy for providing me advices, UNC Lenti-shRNA Core Facility for producing shRNA clones, and Dr. Michelle Itano for confocal microscope troubleshooting. In addition, I would like to thank Dr. Amy Maddox and Kathryn Headley for organizing honors thesis, my fellow honors thesis group members Caroline Minnick and Maggie Cai for peer reviewing, and Dr. Blaire Steinwand for sponsoring my thesis.

This work was supported by a grant from the National Multiple Sclerosis Society (RG1607-25207). I would also like to thank the UNC Office of Undergraduate Research for funding via Summer Undergraduate Research Fellowship.

References

Arnett, H. A., Hellendall, R. P., Matsushima, G. K., Suzuki, K., Laubach, V. E., Sherman, P., & Ting, J. P.-Y. (2002). The protective role of nitric oxide in a neurotoxicant-induced demyelinating model. *Journal of Immunology (Baltimore, Md. : 1950)*, *168*(1), 427–433. https://doi.org/10.4049/JIMMUNOL.168.1.427

Arnett, H. A., Mason, J., Marino, M., Suzuki, K., Matsushima, G. K., & Ting, J. P.-Y. (2001). TNFα promotes proliferation of oligodendrocyte progenitors and remyelination. *Nature Neuroscience*, *4*(11), 1116–1122. https://doi.org/10.1038/nn738

Bever, C. T., & Garver, D. W. (1995). Increased cathepsin B activity in multiple sclerosis brain. *Journal of the Neurological Sciences*, *131*(1), 71–73. Retrieved from http://www.ncbi.nlm.nih.gov/pubmed/7561950

Bever, C. T., Panitch, H. S., & Johnson, K. P. (1994). Increased cathepsin B activity in peripheral blood mononuclear cells of multiple sclerosis patients. *Neurology*, *44*(4), 745–748. Retrieved from http://www.ncbi.nlm.nih.gov/pubmed/8164836

Boutté, A. M., Friedman, D. B., Bogyo, M., Min, Y., Yang, L., & Lin, P. C. (2011). Identification of a myeloid-derived suppressor cell cystatin-like protein that inhibits metastasis. *FASEB Journal : Official Publication of the Federation of American Societies for Experimental Biology*, *25*(8), 2626–2637. https://doi.org/10.1096/fj.10-180604

Cox, J., Hein, M. Y., Luber, C. A., Paron, I., Nagaraj, N., & Mann, M. (2014). Accurate Proteome-wide Label-free Quantification by Delayed Normalization and Maximal

Peptide Ratio Extraction, Termed MaxLFQ. *Molecular & Cellular Proteomics*, *13*(9), 2513–2526. https://doi.org/10.1074/mcp.M113.031591

Cox, J., & Mann, M. (2008). MaxQuant enables high peptide identification rates, individualized p.p.b.-range mass accuracies and proteome-wide protein quantification. *Nature Biotechnology*, *26*(12), 1367–1372. https://doi.org/10.1038/nbt.1511

Cox, J., Michalski, A., & Mann, M. (2011). Software Lock Mass by Two-Dimensional Minimization of Peptide Mass Errors. *Journal of The American Society for Mass Spectrometry*, *22*(8), 1373–1380. https://doi.org/10.1007/s13361-011-0142-8

Dubois-Dalcq, M., ffrench-Constant, C., & Franklin, R. J. M. (2005). Enhancing Central Nervous System Remyelination in Multiple Sclerosis. *Neuron*, *48*(1), 9–12. https://doi.org/10.1016/j.neuron.2005.09.004

Faure, C., Ramos, M., & Girault, J.-A. (2013). Pyk2 cytonuclear localization: mechanisms and regulation by serine dephosphorylation. *Cellular and Molecular Life Sciences*, *70*(1), 137–152. https://doi.org/10.1007/s00018-012-1075-5

Ghasemi, N., Razavi, S., & Nikzad, E. (2017). Multiple Sclerosis: Pathogenesis, Symptoms, Diagnoses and Cell-Based Therapy. *Cell Journal*, *19*(1), 1–10. https://doi.org/10.22074/CELLJ.2016.4867

Gholamzad, M., Ebtekar, M., Ardestani, M. S., Azimi, M., Mahmodi, Z., Mousavi, M. J., & Aslani, S. (2019). A comprehensive review on the treatment approaches of multiple sclerosis: currently and in the future. *Inflammation Research*, *68*(1), 25–38. https://doi.org/10.1007/s00011-018-1185-0

Haves-Zburof, D., Paperna, T., Gour-Lavie, A., Mandel, I., Glass-Marmor, L., & Miller, A. (2011). Cathepsins and their endogenous inhibitors cystatins: expression and modulation in multiple sclerosis. *Journal of Cellular and Molecular Medicine*, *15*(11), 2421–2429. https://doi.org/10.1111/j.1582-4934.2010.01229.x

Hook, G., Jacobsen, J. S., Grabstein, K., Kindy, M., & Hook, V. (2015). Cathepsin B is a New Drug Target for Traumatic Brain Injury Therapeutics: Evidence for E64d as a Promising Lead Drug Candidate. *Frontiers in Neurology*, *6*, 178. https://doi.org/10.3389/fneur.2015.00178

Hsieh, J., Aimone, J. B., Kaspar, B. K., Kuwabara, T., Nakashima, K., & Gage, F. H. (2004). IGF-I instructs multipotent adult neural progenitor cells to become oligodendrocytes. *The Journal of Cell Biology*, *164*(1), 111–122. https://doi.org/10.1083/jcb.200308101

Jones, A. P., Kermode, A. G., Lucas, R. M., Carroll, W. M., Nolan, D., & Hart, P. H. (2017). Circulating immune cells in multiple sclerosis. *Clinical and Experimental Immunology*, *187*(2), 193–203. https://doi.org/10.1111/cei.12878

Kamen, L. A., Schlessinger, J., & Lowell, C. A. (2011). Pyk2 is required for neutrophil degranulation and host defense responses to bacterial infection. *Journal of Immunology (Baltimore, Md. : 1950)*, *186*(3), 1656–1665. https://doi.org/10.4049/jimmunol.1002093

Karamita, M., Barnum, C., Möbius, W., Tansey, M. G., Szymkowski, D. E., Lassmann, H., & Probert, L. (2017). Therapeutic inhibition of soluble brain TNF promotes remyelination by increasing myelin phagocytosis by microglia. *JCI Insight*, *2*(8).

https://doi.org/10.1172/jci.insight.87455

Kotter, M. R., Li, W.-W., Zhao, C., & Franklin, R. J. M. (2006). Myelin Impairs CNS Remyelination by Inhibiting Oligodendrocyte Precursor Cell Differentiation. *Journal of Neuroscience*, *26*(1), 328–332. https://doi.org/10.1523/JNEUROSCI.2615-05.2006

Kotter, M. R., Zhao, C., van Rooijen, N., & Franklin, R. J. M. (2005). Macrophage-depletion induced impairment of experimental CNS remyelination is associated with a reduced oligodendrocyte progenitor cell response and altered growth factor expression. *Neurobiology of Disease*, *18*(1), 166–175. https://doi.org/10.1016/j.nbd.2004.09.019

Lambert, J.-C., Ibrahim-Verbaas, C. A., Harold, D., Naj, A. C., Sims, R., Bellenguez, C., … Amouyel, P. (2013). Meta-analysis of 74,046 individuals identifies 11 new susceptibility loci for Alzheimer's disease. *Nature Genetics*, *45*(12), 1452–1458. https://doi.org/10.1038/ng.2802

Lampron, A., Larochelle, A., Laflamme, N., Préfontaine, P., Plante, M.-M., Sánchez, M. G., … Rivest, S. (2015). Inefficient clearance of myelin debris by microglia impairs remyelinating processes. *The Journal of Experimental Medicine*, *212*(4), 481–495. https://doi.org/10.1084/jem.20141656

Mason, J. L., Ye, P., Suzuki, K., D'Ercole, A. J., & Matsushima, G. K. (2000). Insulin-like growth factor-1 inhibits mature oligodendrocyte apoptosis during primary demyelination. *The Journal of Neuroscience : The Official Journal of the Society for Neuroscience*, *20*(15), 5703–5708. Retrieved from

http://www.ncbi.nlm.nih.gov/pubmed/10908609

Matsushima, G. K., & Morell, P. (2001). The neurotoxicant, cuprizone, as a model to study demyelination and remyelination in the central nervous system. *Brain Pathology (Zurich, Switzerland)*, *11*(1), 107–116. Retrieved from http://www.ncbi.nlm.nih.gov/pubmed/11145196

Menn, B., Garcia-Verdugo, J. M., Yaschine, C., Gonzalez-Perez, O., Rowitch, D., & Alvarez-Buylla, A. (2006). Origin of Oligodendrocytes in the Subventricular Zone of the Adult Brain. *Journal of Neuroscience*, *26*(30), 7907–7918. https://doi.org/10.1523/JNEUROSCI.1299-06.2006

Miron, V. E., Boyd, A., Zhao, J.-W., Yuen, T. J., Ruckh, J. M., Shadrach, J. L., … ffrench-Constant, C. (2013). M2 microglia and macrophages drive oligodendrocyte differentiation during CNS remyelination. *Nature Neuroscience*, *16*(9), 1211–1218. https://doi.org/10.1038/nn.3469

Mort, J. S., & Buttle, D. J. (1997). Cathepsin B. *The International Journal of Biochemistry & Cell Biology*, *29*(5), 715–720. https://doi.org/10.1016/S1357-2725(96)00152-5

Paone, C., Rodrigues, N., Ittner, E., Santos, C., Buntru, A., & Hauck, C. R. (2016). The Tyrosine Kinase Pyk2 Contributes to Complement-Mediated Phagocytosis in Murine Macrophages. *Journal of Innate Immunity*, *8*(5), 437–451. https://doi.org/10.1159/000442944

Scott, R. S., McMahon, E. J., Pop, S. M., Reap, E. A., Caricchio, R., Cohen, P. L., … Matsushima, G. K. (2001). Phagocytosis and clearance of apoptotic cells is

mediated by MER. *Nature*, *411*(6834), 207–211. https://doi.org/10.1038/35075603

Seitz, H. M., Camenisch, T. D., Lemke, G., Earp, H. S., & Matsushima, G. K. (2007). Macrophages and dendritic cells use different Axl/Mertk/Tyro3 receptors in clearance of apoptotic cells. *Journal of Immunology (Baltimore, Md. : 1950)*, *178*(9), 5635–5642. Retrieved from http://www.ncbi.nlm.nih.gov/pubmed/17442946

Siklos, M., BenAissa, M., & Thatcher, G. R. J. (2015). Cysteine proteases as therapeutic targets: does selectivity matter? A systematic review of calpain and cathepsin inhibitors. *Acta Pharmaceutica Sinica B*, *5*(6), 506–519. https://doi.org/10.1016/j.apsb.2015.08.001

Sim, F. J., Zhao, C., Penderis, J., & Franklin, R. J. M. (2002). The age-related decrease in CNS remyelination efficiency is attributable to an impairment of both oligodendrocyte progenitor recruitment and differentiation. *The Journal of Neuroscience : The Official Journal of the Society for Neuroscience*, *22*(7), 2451–2459. https://doi.org/20026217

Snaidero, N., & Simons, M. (2014). Myelination at a glance. *Journal of Cell Science*, *127*(14), 2999–3004. https://doi.org/10.1242/jcs.151043

Takahashi, T., Yamashita, H., Nagano, Y., Nakamura, T., Ohmori, H., Avraham, H., … Matsumoto, M. (2003). Identification and Characterization of a Novel Pyk2/Related Adhesion Focal Tyrosine Kinase-associated Protein That Inhibits α-Synuclein Phosphorylation. *Journal of Biological Chemistry*, *278*(43), 42225–42233. https://doi.org/10.1074/jbc.M213217200

Taylor, L. C., Gilmore, W., Ting, J. P.-Y., & Matsushima, G. K. (2010). Cuprizone

induces similar demyelination in male and female C57BL/6 mice and results in disruption of the estrous cycle. *Journal of Neuroscience Research*, *88*(2), 391–402. https://doi.org/10.1002/jnr.22215

UniProt: a worldwide hub of protein knowledge. (2019). *Nucleic Acids Research*, *47*(D1), D506–D515. https://doi.org/10.1093/nar/gky1049

Zhang, Y., Chen, K., Sloan, S. A., Bennett, M. L., Scholze, A. R., O'Keeffe, S., … Wu, J. Q. (2014). An RNA-sequencing transcriptome and splicing database of glia, neurons, and vascular cells of the cerebral cortex. *The Journal of Neuroscience : The Official Journal of the Society for Neuroscience*, *34*(36), 11929–11947. https://doi.org/10.1523/JNEUROSCI.1860-14.2014